Heliyon 9 (2023) e22382

Contents lists available at ScienceDirect

Heliyon

journal homepage: www.cell.com/heliyon

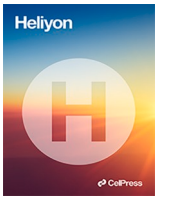

A precise prognostic signature in CTNNB1-mutant hepatocellular carcinoma: Prognosis prediction and precision treatment exploration

Junying Wang, Guangyu Zhu *

Department of Interventional and Vascular Surgery, Zhongda Hospital, Southeast University, Jiangsu, 210009, China

ARTICLE INFO

Keywords:
Prognostic signature
CTNNB1 mutation
Hepatocellular carcinoma
Personalized prognosis management
Precision treatment
Therapeutic target

ABSTRACT

Background: CTNNB1 mutates in most hepatocellular carcinoma (HCC) which is the most familiar form of liver cancer with high heterogeneity. It is critical to create a specific prognostication methodology and to investigate additional treatment options for CTNNB1-mutant HCCs.
Methods: A total of 926 samples in five independent cohorts were enrolled in this study, including 127 CTNNB1-mutant samples and 75 estimated CTNNB1-mutant samples. The prognostic signature was constructed by LASSO-Cox regression and evaluated by bioinformatics analyses. The selection of possible drug targets and agents was produced based on the expression profiles and drug sensitivity data of cancer cell lines in two databases.
Results: A prognostic signature based on 15 genes categorized the CTNNB1-mutant HCCs into two groups with different risks. Compared to low-risk patients, high-risk patients had significantly inferior prognoses. ROC curve and multivariate analysis also indicated the superior performance of our signature on the prognosis estimation, particularly in CTNNB1-mutant HCCs. Besides, the nomogram was constructed according to the prognostic signature with excellent predictive performance confirmed by the calibration curve. Subsequently, we suggested that AT-7519 and PHA-793887 might be potential drug agents for high-risk patients.
Conclusion: We established a 15-gene prognostic model, particularly in HCCs with CTNNB1 mutations with good predictive efficiency. Besides, we explored the potential drug targets and agents for patients with high risk. Our findings offered a fresh idea for personalized prognosis management in HCCs with CTNNB1 mutations and threw new insight for precise treatment in HCCs as well.

1. Introduction

According to the report made by the International Agency for Research on Cancer (IARC), more than nine million people in the world were diagnosed with liver cancer and over 8.3 million people died of it, leading to that liver cancer becoming one of the most frequent cancers in 2020, globally [1]. Notably, nearly half of the death cases were reported in China [2]. Besides, nearly 90 % of cases were diagnosed as hepatocellular carcinoma (HCC) [3]. Although patients with early-stage liver cancer can benefit from liver transplantation and surgical removal with a high 5-year survival rate [4], most of the diagnoses are advanced liver cancers [5]. Thus,

* Corresponding author.
E-mail address: njzgy@sina.com (G. Zhu).

https://doi.org/10.1016/j.heliyon.2023.e22382
Received 1 February 2023; Received in revised form 27 September 2023; Accepted 10 November 2023
Available online 14 November 2023

extremely poor outcomes were commonly found in patients with liver cancer. As the research on mechanism of liver cancer moves along, the mutation of many genes in liver cancer has been illuminated to be a contributor of the development of liver cancer [6]. Of which, mutations in the CTNNB1 gene are one of the most frequent genetic events in HCC [7].

CTNNB1, a mutant in 20%–40 % of liver tumors, encodes β-catenin which is central in the canonical WNT signaling pathway acting as an intracellular signal transducer [8]. The Wnt signaling pathway regulates cellular proliferation, embryonic development, and cellular differentiation in a tightly controlled and highly conserved manner [9]. Recently, there are two different Wnt signaling pathways have been identified, termed non-canonical and canonical pathways. Of note, increasing evidence has illustrated the crucial role of Wnt/β-catenin signaling in the carcinogenesis and progression of liver cancer [10]. Besides, increasing studies have illuminated that HCC can achieve immune evasion by activating β-catenin resulting in resistance to *anti*-PD-1 therapies [11], and liver cancer with CTNNB1 mutation was associated with T cell exclusion [12]. Therefore, precision treatment of liver cancer with CTNNB1 mutation is still a challenge.

In this study, our aim is to establish a prognostic signature for liver cancer patients with CTNNB1 mutation and to excavate the latent therapeutic spots and drugs. Multiple datasets were collected and we first established a prediction model to estimate the CTNNB1 mutation status of samples lacking mutation status information. The samples with CTNNB1 mutation were extracted and used to develop a prognostic molecular signature. And then, the prognostic model was analyzed by multiple methods to test the accuracy and dependence in the prognosis prediction of CTNNB1-mutant HCC. In addition, we sought the possible drug targets and agents in mutant-CTNNB1 HCCs with high risk. We hope that this study could provide a new strategy for personalized prognostic monitoring in HCCs with CTNNB1 mutations, and offer new clues for precision therapies in CTNNB1-mutant HCCs.

2. Methods

2.1. Data collection and preprocessing

Two RNA-sequencing cohorts with transcriptome profiles and complete clinical information were enrolled from The Cancer Genome Atlas Liver Hepatocellular Carcinoma (TCGA-LIHC) cohort (version: 07-19-2019), and the data was downloaded from the TCGA database (https://portal.gdc.cancer.gov). Besides, the somatic mutation data of 373 samples were obtained and downloaded from the cBioPortal website (https://www.cbioportal.org/). Finally, 363 samples with somatic mutation data and survival data were enrolled for further analysis and the clinical features of these samples were summarized in Supplementary Table 1. Paired tumor and non-tumor liver tissues of 159 HCC samples with hepatitis B virus (HBV) infection who underwent primary curative resection in the CHCC-HBV cohort was obtained at Zhongshan Hospital (Fudan University, Shanghai, China) between 2010 and 2014. The RNA-sequencing data was downloaded from the National Omics Data Encylopedia (NODE) database (https://www.biosino.org/node). Clinical and molecular data of the CHCC-HBV cohort was obtained from the supplementary files of reference [13] and summarized in Supplementary Table 2. After removing the batch effect, the TCGA-LIHC cohort and the CHCC-HBV cohort were integrated into one cohort for further analysis (Supplementary Fig. 1A).

This study further enrolled three microarray cohorts, including 64 HCC samples in the GSE116174 cohort, 242 HCC samples in the GSE14520 cohort, and 115 HCC samples in the GSE76427 cohort. The expression matrix and clinical information were downloaded from the Gene Expression Omnibus (GEO) database (http://www.ncbi.nlm.nih.gov/geo/). For the two cohorts (GSE14520 and GSE116174) based on the GPL3921 platform and GPL13158 platform, raw sequencing data were normalized by the RMA method implemented in the *affy* R package [14]. For the GSE76427 cohort based on the GPL10558 platform, the robust spline normalization (RSN) method was used to normalize the matrix data by the *lumi* R package. After removing the batch effect, three GEO cohorts were combined into one GEO cohort (Supplementary Fig. 1B). The clinical features of the combined GEO cohort were summarized in Supplementary Table 3.

Cancer cell line information including expression profiles and somatic mutation were obtained from the Broad Institute-Cancer Cell Line Encyclopedia (CCLE) database. We determined how dependent a gene is in the CTNNB1-mutant HCC cell line by comparing the cancer-dependent score (CERES score) of each gene obtained from the dependency map (DepMap) portal (https://depmap.org/portal/). CERES is an indicator to reflect the perturbation effect of specific gene in a certain cell line analyzed by using CRISPR-Cas9 [15,16]. A negative score represents that knocking down the certain gene inhibits the cell line growth, on the other hand, a positive score reflected that the cell line growth is promoting after knocking down the certain gene [17,18]. It is widely accepted that a gene with a lower CERES score suggests that the gene has a higher possibility to be crucial in cell growth and survival.

2.2. CTNNB1-mutation prediction model construction

We noticed no record of the mutation status of CTNNB1 in the clinical information of the combined GEO cohort. To achieve a more reliable result, Randomforests (RFs) method was used to construct a model to estimate the status of CTNNB1 mutation. RFs is an ensemble learning method and is mainly based on the combination of several independent decision trees. Among them, each tree depends on the value of an independently sampled random vector, and the distribution is the same for all trees in the forest [19,20]. RFs develop a model by building up multiple decision trees whose results will be counted and voting for the final result selection when predicting a certain sample. The RFs algorithm has been applied in pattern recognition successfully [21]. We first randomized the CTNNB1-mutant HCCs in the combined RNA-seq cohort into two sets equally. RFs method was producted by using the R package "RandomForest" in the training set to construct a prediction model and the testing set to validate the predictive efficiency. Finally, we estimated the status of CTNNB1 mutations by using the prediction model in the combined GEO cohort, and the estimated

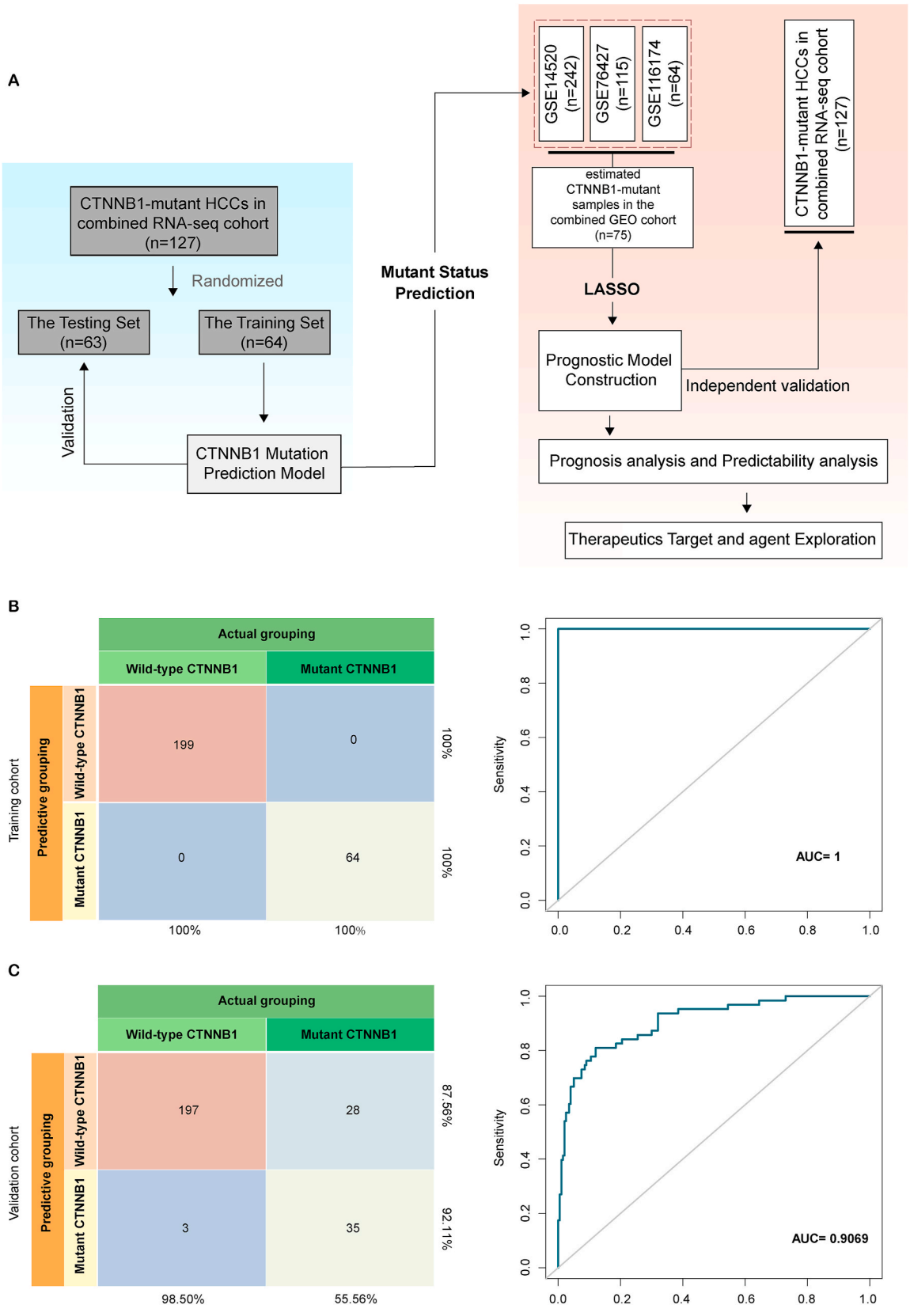

Fig. 1. The flow chart of this study (A) and CTNNB1 mutation status prediction model in the training set and the testing set (B).

CTNNB1-mutant HCCs were enrolled for further analysis.

2.3. Establishment of prognostic model in CTNNB1-mutant HCC

The prognostic value of the gene was evaluated by using univariate-cox analysis in the estimated CTNNB1-mutant patients in the combined GEO cohort, and genes that had significant prognostic value in the estimated CTNNB1-mutant samples ($p < 0.05$) were extracted for further analysis. The estimated CTNNB1-mutant patients in the GEO cohort were separated into the training set and the testing set equally and randomly. The signature based on the extracted prognostic genes was established using The Least Absolute Shrinkage and Selection Operator (LASSO)-Cox method [22,23] which was implemented in the "glmnet" R package [24] in the training set. The testing set was employed as internal validation, and the CTNNB1-mutant HCCs in the combined RNA-seq cohort were employed as independent external validation.

2.4. Exploration of potential therapeutic targets in high risk CTNNB1-mutant HCC

The druggable genes were collected from the Drug Gene Interaction (DGI) database. Firstly, we calculated the correlation between the risk score and the expression level of the druggable proteins using the Pearson's correlation analysis. The druggable proteins that significantly correlated with the risk score were selected as candidate targets with criteria of correlation coefficient >0.3 and p-value <0.05. Subsequently, the CERES score of the candidate targets in the CTNNB1-mutant hepatoma cell line (SNU-398) was obtained from the CCLE database. Candidate protein targets were defined as essential protein targets with a CERES score of less than 0.

2.5. Drug sensitivity analysis

Genomics of drug sensitivity in cancer (GDSC) is the largest public resource for information on drug sensitivity in cancer cells and molecular markers of drug response [25]. The drug susceptibility data of 518 antineoplastic agents across almost 1000 cancer cell lines were obtained from the GDSC database (www.cancerRxgene.org). The corresponding drugs targeted to the selected essential protein genes were used for further drug susceptibility analysis by comparing the half-maximal inhibitory concentration (IC50) of the corresponding drugs in the hepatoma cell line with CTNNB1 mutation (SNU-398) to identify potential drugs for high-risk patients with CTNNB1 mutation. IC50 represents drug concentration eliciting 50 % of the maximum inhibition, which is an important pharmacodynamic index of drug effectiveness. The drug with lower IC50 is defined as more sensitive to the specific cell line.

2.6. Statistical analysis

Survival analysis was performed by using the "survival" R package and visualized by using the R package "survminer". The difference significance between the two groups was calculated by using the log-rank test. The area under the receiver operating characteristic (ROC) curve (AUC) and the concordance index (*C*-index) was calculated by using the R package "timeROC" and the "pec" respectively to test the robustness of the prognostic signature. "Rms" R package was applied to construct the Nomogram and the calibration curve. All the statistical analysis and visualization were conducted with the corresponding R package of R (version 4.0.2). There is a significant significance when the p-value is less than 0.05. The flow chart of this study was shown in Fig. 1A.

3. Results

3.1. A robust model for CTNNB1 mutation status prediction

The CTNNB1-mutant patients in the RNA-seq cohort were randomly divided into the training set and the testing set with a ratio of 1:1. We constructed a prediction model by using RFs in the training set. And then, we tested the predictability of the model in the training set. We found that 100 % of samples with mutant-CTNNB1 were distinguished from the CTNNB1 wild-type samples with the AUC = 1.00 (Fig. 1B). Besides, the model could predict the CTNNB1 mutation status with an AUC = 0.9069 when validating the model in the testing set (Fig. 1C). Moreover, we validated the RF prediction model by comparing it with the model constructed by the K-Nearest Neighbor (KNN) method, and the result showed that the performance of the KNN prediction model only achieved AUC = 0.7515 in the testing set (Supplementary Fig. 2), which suggested that the RF prediction model had better predictive efficiency compared to the KNN prediction model. Taken together, we indicated that the efficiency of the RF prediction model was very good and could be used for CTNNB1 mutation prediction in other cohorts. Subsequently, we predicted the CTNNB1 mutant status of the HCC patients in the GEO cohort. Finally, seventy-five samples were estimated as CTNNB1-mutant and extracted for follow-up analysis.

3.2. Development of a molecular prognostic signature in CTNNB1-mutant HCCs

We identified 509 prognostic-related genes by using single-factor analysis in the estimated CTNNB1-mutant cohort (Supplementary Table 4, $p < 0.05$). And then, Seventy-five estimated CTNNB1-mutant cohort was separated into two sets and one set for signature development and the other for internal validation. A prognostic signature was established by using the LASSO method based on 15 genes, including ARNT, ASPHD1, DYSF, GGA2, ITPA, PPFIA2, PTDSS1, RAB11FIP2, RPL3, RPS12, SLC16A4, SMPD2, TAC3, TNFRSF25, ZNF467 (Supplementary Figs. 3A–3B). And then, the expression patterns of these 15 genes in the GEO cohort showed that

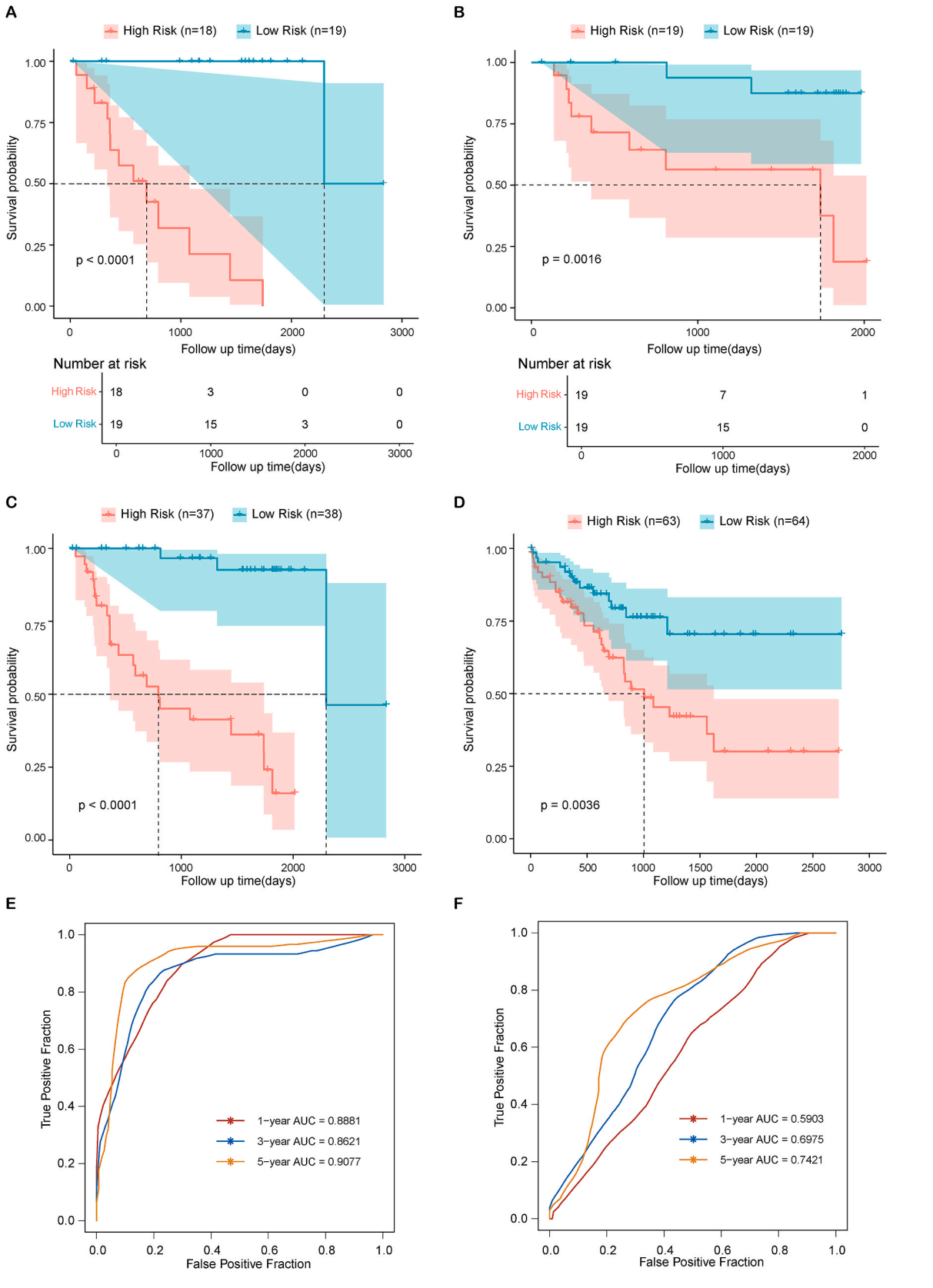

(caption on next page)

Fig. 2. Evaluation and validation of the 15-gene prognostic model. Kaplan-Meier survival curves between the high risk group and the low risk group on the mutant-CTNNB1 samples in the training set (A), the testing set (B), the internal validation cohort (C), and the external validation cohort (D). The red line represents the high risk group while the blue line represents the low risk group. The ROC curve of 1-year (red line), 3-year (blue line), and 5-year (yellow line) survival on the mutant-CTNNB1 samples in the combined GEO cohort (E) and the combined RNA-seq cohort (F).

most of these 15 genes tended to dysexpression in the CTNNB1-mutant samples (Supplementary Fig. 3C). Besides, we further compared the expression level of the signature genes between CTNNB1-mutant samples and CTNNB1 wild-type patients in the RNA-seq cohort. The result indicated that the expression level of GGA2, SMPD2, ARNT, TAC3, ASPHD1, ZNF467, and TNFRSF25 was significantly higher in samples with CTNNB1 mutations while significantly lower expression of RAB11FIP2 and SLC16A4 was found in samples with CTNNB1 mutations (Supplementary Fig. 4), which further suggested that our signature might be associated with CTNNB1 mutations in HCCs. Subsequently, the association between the 15 signature genes and CTNNB1 on the expression level was analyzed. We found that RAB11FIP2 was the most positively correlated with CTNNB1 while TAC3 was the most negatively correlated with CTNNB1 (Supplementary Fig. 3D). Besides, the association between the 15 genes and the CTNNB1 gene was also analyzed on the functional level using the "GOSemSim" R package [26] and we found that RAB11FIP2 had the most similar function with CTNNB1 in HCC samples (Supplementary Fig. 3E), which indicated that RAB11FIP2 might be the key gene in the CTNNB1-mutant HCC. And then, we calculated the risk score of each CTNNB1-mutant sample enrolled in this study by using the unified formula (Supplementary Table 5). Subsequently, samples in each set were separated into different risk groups based on the median value of risk scores, severally.

3.3. *Performance of our prognostic signature in CTNNB1-mutant HCCs*

Clinical features comparison showed that the difference between high-risk and low-risk groups was not significant in both the estimated CTNNB1-mutant samples of the combined GEO cohort and actual CTNNB1-mutant samples of the combined RNA-seq cohort (Supplementary Tables 6–7). Survival analysis suggested that a high risk score was associated with inferior overall survival significantly in the training set (Fig. 2A, $p < 0.0001$) and the testing set (Fig. 2B, $p = 0.0016$). Subsequently, the performance of our signature was validated in the CTNNB1-mutant samples of the GEO cohort with a larger sample size. The result suggested that a high risk score portended an inferior prognosis (Fig. 2C, $p < 0.0001$), and 5-year AUC value was larger than 0.9 in the GEO cohort (Fig. 2E). Moreover, we performed principal components analysis (PCA) and t-distributed stochastic neighbor embedding (*t*-SNE) analysis in the estimated CTNNB1-mutant cohort. The result suggested that our signature still could also provide discrimination using unsupervised methods (Supplementary Fig. 5). In addition, we enrolled one hundred and twenty-seven CTNNB1-mutant HCCs in the combined RNA-seq

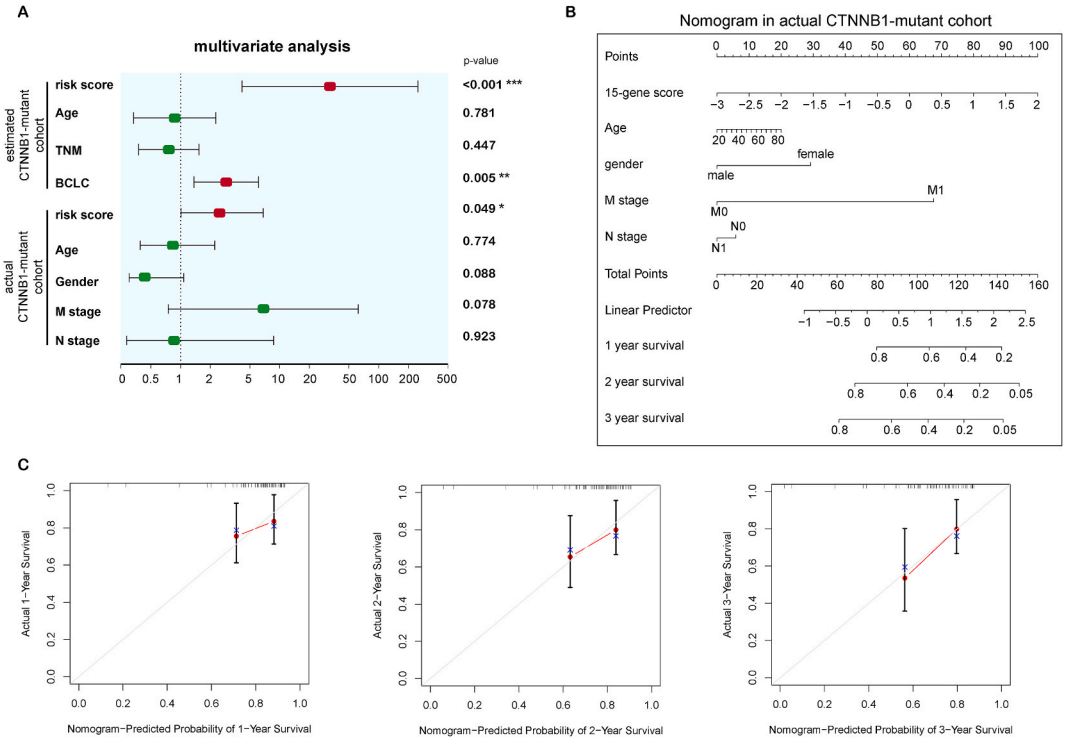

Fig. 3. Evaluation of the 15-gene prognostic model. (A) Multivariate analysis was performed in the CTNNB1-mutant samples of both the GEO cohort and the RNA-seq cohort. (B) The nomogram based on the 15-gene prognostic model and other clinical features in the CTNNB1-mutant samples of the combined RNA-seq cohort was constructed. (C) Calibration curves.

cohort as external validation. Notably, increasing risk score was relevant to shorter survival time (Fig. 2D, p = 0.0036), and the 5-year AUC value was 0.7424 in the combined RNA-seq cohort (Fig. 2F), which provided a more explicit hint that the 15-gene prognostic signature had great efficiency in the prediction of prognosis in CTNNB1-mutant HCCs. Whereafter, multivariate-cox analysis was performed to test the prognostic value independent of the 15-gene signature in CTNNB1-mutant HCCs. The risk score based on the fifteen signature genes was an independent poor prognostic factor in CTNNB1-mutant HCCs (Fig. 3A). Furthermore, we fabricated the nomogram based on the risk score and multiple clinicopathological parameters in the CTNNB1-mutant HCCs (Fig. 3B, Supplementary Fig. 6A). The efficiency of the nomogram was further tested by the calibration curve. Unsurprisingly, our nomogram had great efficiency in the prediction of prognosis in the CTNNB1-mutant HCCs (Fig. 3C, Supplementary Fig. 6B). Complementarily, we calculated the risk score and performed the prognosis analysis on both the CTNNB1 wild-type HCCs. The result indicated that the 15-gene prognostic signature failed to keep a good predictive efficiency in CTNNB1 wild-type HCCs (Supplementary Fig. 7).

3.4. Exploration of possible drug targets and agents in CTNNB1-mutant HCCs with high risk

As described in methods, we performed a two-step analysis to identify the potential therapeutic targets that associated with the risk score, which was depicted as flow chart intuitively (Fig. 4A). Firstly, according to the filter criteria described in the method (correlation coefficient>0.3 and p-value<0.05), 653 druggable protein-coding genes were selected as candidate targets (Supplementary Table 8). Subsequently, the CERES scores of these candidate targets in SNU-398 cell line were collected and the candidate targets with CERES score less than 0 were identified as essential targets. Finally, 251 druggable protein-coding genes were identified as essential targets in the CTNNB1-mutant HCCs (Fig. 4B, Supplementary Table 9).

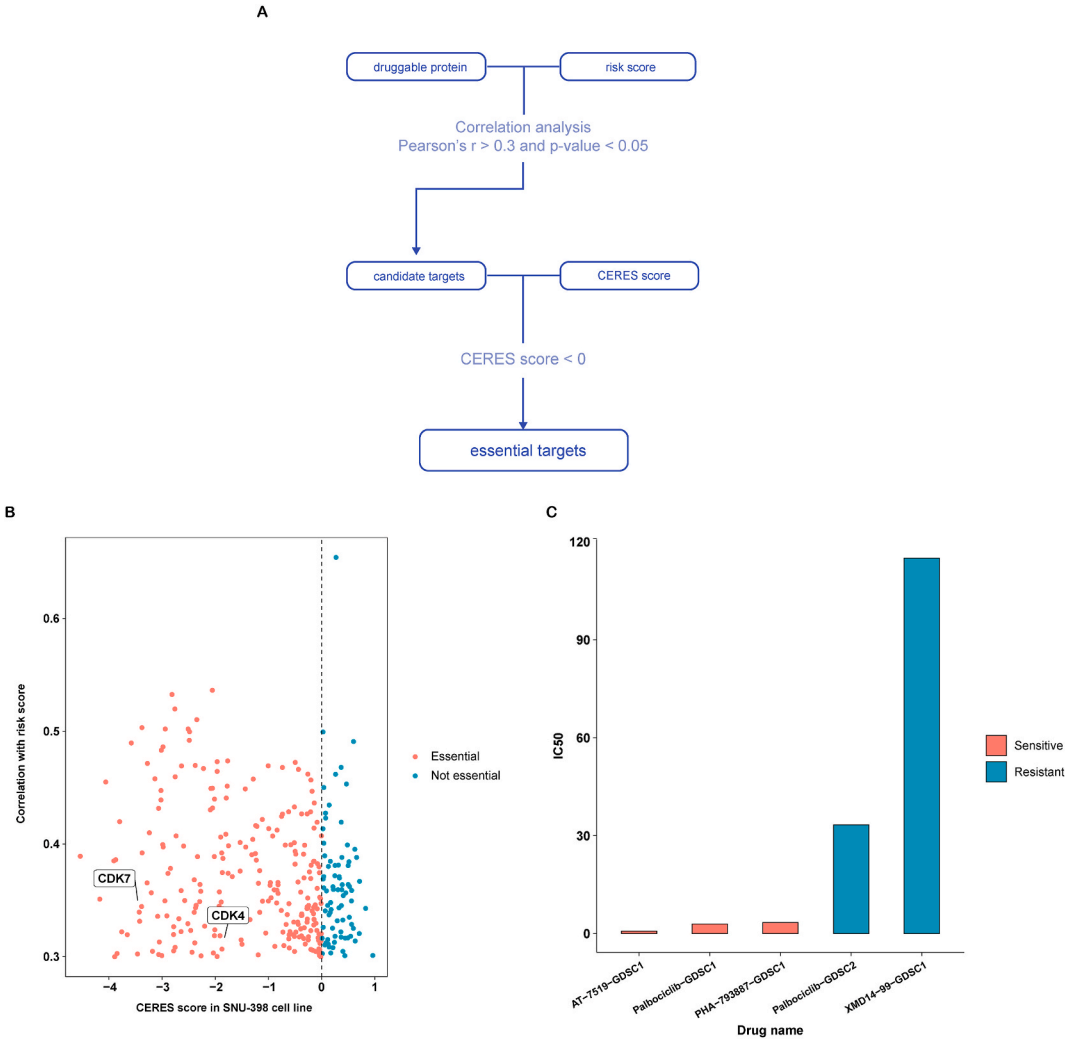

Fig. 4. Exploration of potential targets and agents for high risk samples. (A) A flow chart of the potential targets selection process. (B) Correlation coefficient and CERES score of candidate targets. Red dot represents the essential target and blue dot represents the non-essential target. (C) IC50 of the sensitive drugs in CNU-398 cell line in GDSC1 dataset. (D) IC50 of the sensitive drugs in CNU-398 cell line in GDSC2 dataset.

Moreover, we collected the IC50 of 518 anti-tumor drugs in the CTNNB1-mutant HCC cell line (SNU-398) from two datasets (GDSC1 and GDSC2) in the GDSC database. We searched the corresponding drugs of the essential targets and only two of the essential targets had its corresponding drug, including four drugs in the GDSC1 dataset (AT-7519, Palbociclib, PHA-793887, XMD14-99) and one drug (Palbociclib) in the GDSC2 dataset. Afterwards, we compared the IC50 of 5 drugs in SNU-398 cell line (Supplementary Table 10). As shown in Fig. 4C, the SNU-398 cell line was sensitive to AT-7519, Palbociclib, and PHA-793887 in the GDSC1 dataset. However, palbociclib was not effective to the SNU-398 cell line in the GDSC2 dataset. Besides, the SNU-398 cell line cannot be suppressed after treating with XMD14-99. Taken together, AT-7519 and PHA-793887 might be the potential antineoplastic agents for CTNNB1-mutant HCCs with high risk. Moreover, we further identified the potential agents targeted to other protein/pathway except for the target we selected for CTNNB1-mutant HCCs in the GDSC database. We found that the SNU-398 cell line was sensitive to 146 agents including the agents we identified above (Supplementary Table 11), providing novel thought for clinical application of these 146 agents in CTNNB1-mutant HCCs.

4. Discussion

It is well-known that as the most common form of liver cancer, HCC is an extraordinarily heterogeneous tumor at both the molecular and histological level. Nowadays, many clinical factors have been illustrated that might affect the prognosis of HCC mostly because of the complicacy of the pathogenesis in HCC. Therein, HBV/HCV infection is one of the most important risk factor. Many studies have illuminated that suppressing viral load improves HCC prognosis [27]. Besides, liver function is another important factor for HCC prognosis since hepatic failure is one of the most severe complications in HCC. HCC accompanied by more severe liver function injury had worse prognosis. In addition, treatment options might also affect the prognosis of HCC. Surgical resection is the most curative option for early-stage HCC with very good prognosis but not for advanced disease [28]. Radiofrequency ablation (RFA) and Trans arterial chemoembolization (TACE) are treatments approved to be used in advanced HCCs [29]. However, low efficiency and high rate of resistance are hard to overcome. In the molecular level, several transcriptomic-based HCC subtypes have been identified recently. Overall, a system was developed to divide HCC into two major groups [7]. HCCs that have a well-differentiated phenotype with activation of the Wnt/β-catenin pathway as main molecular feature were classified into one group. HCCs in the other group shows activation of signaling pathways contributed in cell cycle progression leading to a more aggressive phenotype. CTNNB1 gene encodes β-catenin, the central hub in the Wnt signaling pathway [30], and mutation of which is one of the most frequent alterations in HCC [31]. Although some studies have demonstrated that CTNNB1 mutations in HCCs was associated with well-differentiated tumors [12], the other studies illustrated that activation of Wnt/β-catenin cascade has been linked to tumor progression and had inferior prognosis comparing to CTNNB1 wild-type patients, which indicated that the relationship between β-catenin activation and HCC patient survival remains controversial [32,33]. It is critical to provide personalized therapy approach for these patients. In this study, a prognostic signature was established based on 15 genes (ARNT, ASPHD1, DYSF, GGA2, ITPA, PPFIA2, PTDSS1, RAB11FIP2, RPL3, RPS12, SLC16A4, SMPD2, TAC3, TNFRSF25, and ZNF467) in CTNNB1-mutant HCCs, showing excellent efficiency on the prediction of prognosis in mutant-CTNNB1 HCCs. Furthermore, we explored the possible drug targets and agents in mutant-CTNNB1 HCCs, which provided new ideas for achieving precision treatment in HCC patients with CTNNB1 mutation.

We found that RAB11FIP2 was the most associated with CTNNB1 on both the expression and functional level among the 15 genes, which suggested that RAB11FIP2 might be the key gene in the CTNNB1-mutant HCCs. RAB11 Family Interacting Protein 2 (RAB11FIP2) participates in cell polarity maintaining and establishment, polarized structures construction or cargo distribution during cytokinesis by interacting with Rab11 [34]. Many researches have illuminated the regulation function of RAB11FIP2 in the migration and invasion of cancer cells. However, the role of RAB11FIP2 in HCC has not been investigated. Therefore, our findings provided a new clue to investigating the role of RAB11FIP2 in liver cancer. In addition, some genes among the 15 genes have been reported that was associated with the development of liver cancer. For example, Aryl hydrocarbon receptor nuclear translocator (ARNT), namely hypoxia-inducible factor 1β(HIF1β), plays an important part in metabolism control in liver [35]. Besides, ARNT not only is an important regulator of HCC growth and metastasis but also regulates anti-tumor effects under hypoxic conditions in HCCs [36–38]. Golgi-localized, γ-adaptin ear-containing, ADP ribosylation factor-binding protein 2 (GGA2) is a member of ADP ribosylation factor (ARF)-dependent monomeric clathrin adaptors family. Previous studies have demonstrated that GGAs interacts with EGFR for maintaining the receptor expression resulting in supporting cell growth [39,40]. Solute Carrier Family 16 Member 4 (SLC16A4, so-called MCT4) is a high-affinity lactate transporter with physiologically relevant affinity for pyruvate [41]. Previous studies have illuminated that overexpression of MCT4 is usually found in a large-scale of HCCs and associated with poor prognosis in HCCs [42]. Besides, blocking MCT4 confers self-regulated apoptosis by disrupting intracellular pH homeostasis in HCCs [43].

CERES score is an assessment indicator to reflect the importance of genes for survival of cancer cell lines. The lower CERES score indicates a promote effect of the certain gene for cell growth. The genes that were positively correlated with risk score at the expression level and with CERES score <0 at the same time were identified as potential targets for high risk patients. Therefore, we found 251 druggable proteins as essential targets. Some essential targets have strong competitiveness to become the therapeutic target for high risk patients, such as PES1 (correlation coefficient = 0.52, CERES score = −2.76) and RPS11 (correlation coefficient = 0.47, CERES score = −3.27). Pescadillo, encoded by PES1, is a nuclear protein that is involved in multiple biological processes including DNA replication, cell cycle progression, ribosome synthesis and embryonic development [44,45]. Some studies have illuminated that PES1 promotes tumorigenesis in HCC and is a poor prognostic biomarker for liver cancer [46,47]. RPS11 is a member of ribosomal protein family which participates in cell cycle, tumorigenesis, proliferation, apoptosis and DNA repair [48]. A study has demonstrated that RPS11 acted as a potential prognostic biomarker in HCCs [49]. Therefore, our findings further provided insightful clues for novel therapeutic targets for mutant-CTNNB1 HCCs.

It is well-acknowledge that the best way to discover a new drug is to start with an old one. Discovery of the new indications and application of the drugs that were approved by FDA or were on-going the clinical trials not only reduces the research and development cost but also promotes the therapy development [50]. Thus, we screened the therapeutic agents that targeted to our selected essential targets in the GDSC database, the largest anti-tumor drug sensitivity public database globally. Our findings suggested that the CTNNB1-mutant HCC cell line was sensitive to AT-7519 and PHA-793887. AT-7519 and PHA-793887 are both pan-Cyclin-Dependent Kinase (CDK) inhibitors. CDKs are known to be important regulators of cell cycle progression. In HCC, CDK7 activates beta-catenin/TCF signaling resulting in promoting cell growth and migration as a therapeutic target in HCCs [51], which was consistent with our finding. In the last 20 years, many agents targeting CDK enzyme activity have emerged and been evaluated clinically, including AT-7519 and PHA-793887 [52]. Some phase I studies have revealed the preliminary anti-cancer activity of AT-7519 in cancer patients [53–55]. Besides, a recent research has demonstrated that AT-7519 had anti-tumor activity in HCC [56]. Together with our findings, we provided new direction for clinic to further investigate the activity of AT-7519 in patients with CTNNB1-mutant HCC. Besides, a phase I study published in 2011 investigated that PHA-793887 induces severe, dose-related hepatic toxicity [57]. However, some latest studies have revealed the effective role of PHA-793887 in against osteosarcoma [58], lung cancer [59], prostate cancer [60] and ovarian cancer [61]. Therefore, our findings provided new application of PHA-793887 in HCC and theoretical basis for promoting the clinical application of PHA-793887 in CTNNB1-mutant HCC. Additionally, some studies further revealed that CDK played a role in antiviral innate immunity and antitumor immunity [62–64]. HBV infection has been widely recognized as one of the most important high-risk factor for HCC because it can lead to abnormal immune attack in liver mediating chromic liver damage which might result in HCC [65]. Moreover, CTNNB1-mutant HCC was associated with immune exclusion [66, 67]. Therefore, our findings further suggested that CDK might participate in the HBV-induced immune imbalance in CTNNB1-mutant HCCs. Moreover, recent studies have demonstrated that CDK inhibitors can significantly improve the immunotherapy effect in many type of cancer [64,68]. Our findings provided basis on the clinical application of CDK inhibitors and immunotherapies combination therapy in CTNNB1-mutant HCCs.

Nevertheless, some limitations are also occurred in this study. Firstly, HCCs with both transcriptome data and mutation data is very restricted. We predicted the CTNNB1 mutation status in some patients without the data of CTNNB1 mutation status by machine learning method to expand the cohort size and improve the reliability of this study. However, slight discrepancy between estimated and actual CTNNB1 mutation status of these samples might be appeared. Secondly, our findings were all derived from the bioinformatics analyzes, and validating our findings with experiments and clinical trials is advantaged for promoting our findings in clinical application.

5. Conclusion

We established a 15-gene prognostic signature with good performance on prognosis prediction particularly in CTNNB1-mutant HCCs. Our findings proposed a new strategy for personalized prognosis management and threw insights into precise therapy development for CTNNB1-mutant HCCs.

Ethics approval and consent to participate

Not Applicable.

Consent for publication

Not Applicable.

Funding

Not applicable.

Data availability statement

The data in this study was available in the TCGA database the NODE database and the GEO database. (https://portal.gdc.cancer.gov; https://www.biosino.org/node; http://www.ncbi.nlm.nih.gov/geo/).

CRediT authorship contribution statement

Junying Wang: Conceptualization, Data curation, Formal analysis, Investigation, Methodology, Resources, Software, Validation, Visualization, Writing - original draft. **Guangyu Zhu:** Conceptualization, Data curation, Funding acquisition, Project administration, Supervision, Writing - review & editing.

Declaration of competing interest

The authors declare that they have no known competing financial interests or personal relationships that could have appeared to

influence the work reported in this paper.

Acknowledegement

We thank the support of Zhongda Hospital of Southeast University in this project.

Appendix A. Supplementary data

Supplementary data to this article can be found online at https://doi.org/10.1016/j.heliyon.2023.e22382.

References

[1] H. Sung, et al., Global cancer statistics 2020: GLOBOCAN estimates of incidence and mortality worldwide for 36 cancers in 185 countries, CA A Cancer J. Clin. 71 (3) (2021) 209–249.
[2] J.L. Petrick, et al., International trends in hepatocellular carcinoma incidence, 1978-2012, Int. J. Cancer 147 (2) (2020) 317–330.
[3] J.M. Llovet, et al., Hepatocellular carcinoma, Nat. Rev. Dis. Prim. 7 (1) (2021) 6.
[4] P.R. Scherber, et al., [Early stage liver cancer : hepatocellular carcinoma], Chirurg 89 (4) (2018) 281–288.
[5] J.L. Raoul, et al., Updated use of TACE for hepatocellular carcinoma treatment: how and when to use it based on clinical evidence, Cancer Treat Rev. 72 (2019) 28–36.
[6] J. Zucman-Rossi, et al., Genetic landscape and biomarkers of hepatocellular carcinoma, Gastroenterology 149 (5) (2015) 1226–1239 e4.
[7] J. Calderaro, et al., Histological subtypes of hepatocellular carcinoma are related to gene mutations and molecular tumour classification, J. Hepatol. 67 (4) (2017) 727–738.
[8] R. Nusse, H. Clevers, Wnt/beta-Catenin signaling, disease, and emerging therapeutic modalities, Cell 169 (6) (2017) 985–999.
[9] Z. Steinhart, S. Angers, Wnt signaling in development and tissue homeostasis, Development 145 (11) (2018).
[10] S. He, S. Tang, WNT/beta-catenin signaling in the development of liver cancers, Biomed. Pharmacother. 132 (2020), 110851.
[11] M. Ruiz de Galarreta, et al., Beta-catenin activation promotes immune escape and resistance to anti-PD-1 therapy in hepatocellular carcinoma, Cancer Discov. 9 (8) (2019) 1124–1141.
[12] R. Pinyol, D. Sia, J.M. Llovet, Immune exclusion-wnt/CTNNB1 class predicts resistance to immunotherapies in HCC, Clin. Cancer Res. 25 (7) (2019) 2021–2023.
[13] Q. Gao, et al., Integrated proteogenomic characterization of HBV-related hepatocellular carcinoma, Cell 179 (2) (2019) 561–577 e22.
[14] L. Gautier, et al., affy–analysis of Affymetrix GeneChip data at the probe level, Bioinformatics 20 (3) (2004) 307–315.
[15] R.M. Meyers, et al., Computational correction of copy number effect improves specificity of CRISPR-Cas9 essentiality screens in cancer cells, Nat. Genet. 49 (12) (2017) 1779–1784.
[16] A. Tsherniak, et al., Defining a cancer dependency map, Cell 170 (3) (2017), 564-576 e16.
[17] B. Shi, et al., Characteristics and prognostic value of potential dependency genes in clear cell renal cell carcinoma based on a large-scale CRISPR-Cas9 and RNAi screening database DepMap, Int. J. Med. Sci. 18 (9) (2021) 2063–2075.
[18] J. Zhang, et al., MCM2-7 in clear cell renal cell carcinoma: MCM7 promotes tumor cell proliferation, Front. Oncol. 11 (2021), 782755.
[19] J. Sun, et al., Banzhaf random forests: cooperative game theory based random forests with consistency, Neural Network. 106 (2018) 20–29.
[20] S. Carbo-Valverde, P. Cuadros-Solas, F. Rodriguez-Fernandez, A machine learning approach to the digitalization of bank customers: evidence from random and causal forests, PLoS One 15 (10) (2020), e0240362.
[21] Y.W. Wan, B. Zhu, Abnormal patterns recognition in bivariate autocorrelated process using optimized random forest and multi-feature extraction, ISA Trans. 109 (2021) 102–112.
[22] J. Friedman, T. Hastie, R. Tibshirani, Regularization paths for generalized linear models via coordinate descent, J. Stat. Software 33 (1) (2010) 1–22.
[23] N. Simon, et al., Regularization paths for cox's proportional hazards model via coordinate descent, J. Stat. Software 39 (5) (2011) 1–13.
[24] S. Engebretsen, J. Bohlin, Statistical predictions with glmnet, Clin. Epigenet. 11 (1) (2019) 123.
[25] W. Yang, et al., Genomics of Drug Sensitivity in Cancer (GDSC): a resource for therapeutic biomarker discovery in cancer cells, Nucleic Acids Res. 41 (2013) D955–D961. Database issue).
[26] G. Yu, et al., GOSemSim: an R package for measuring semantic similarity among GO terms and gene products, Bioinformatics 26 (7) (2010) 976–978.
[27] M. Harputluoglu, B.I. Carr, Hepatitis B before and after hepatocellular carcinoma, J. Gastrointest. Cancer 52 (4) (2021) 1206–1210.
[28] G.A. Vitiello, et al., Surgical resection of early stage hepatocellular carcinoma improves patient survival at safety net hospitals, J. Surg. Oncol. 123 (4) (2021) 963–969.
[29] E. Chakraborty, D. Sarkar, Emerging therapies for hepatocellular carcinoma (HCC), Cancers 14 (11) (2022).
[30] F. Belinky, et al., PathCards: Multi-Source Consolidation of Human Biological Pathways, Database, Oxford, 2015, 2015.
[31] K. Schulze, et al., Exome sequencing of hepatocellular carcinomas identifies new mutational signatures and potential therapeutic targets, Nat. Genet. 47 (5) (2015) 505–511.
[32] C. Xu, et al., beta-Catenin signaling in hepatocellular carcinoma, J. Clin. Invest. 132 (4) (2022).
[33] L. Chen, et al., CTNNB1 alternation is a potential biomarker for immunotherapy prognosis in patients with hepatocellular carcinoma, Front. Immunol. 12 (2021), 759565.
[34] L.M. Machesky, Rab11FIP proteins link endocytic recycling vesicles for cytoskeletal transport and tethering, Biosci. Rep. 39 (1) (2019).
[35] X.L. Wang, et al., Ablation of ARNT/HIF1beta in liver alters gluconeogenesis, lipogenic gene expression, and serum ketones, Cell Metabol. 9 (5) (2009) 428–439.
[36] Y. Liang, et al., Aryl hydrocarbon receptor nuclear translocator is associated with tumor growth and progression of hepatocellular carcinoma, Int. J. Cancer 130 (8) (2012) 1745–1754.
[37] S.H. Choi, et al., Silencing of hypoxia-inducible factor-1beta induces anti-tumor effects in hepatoma cell lines under tumor hypoxia, PLoS One 9 (7) (2014), e103304.
[38] W. Li, et al., Downregulation of ARNT2 promotes tumor growth and predicts poor prognosis in human hepatocellular carcinoma, J. Gastroenterol. Hepatol. 30 (6) (2015) 1085–1093.
[39] T. Uemura, S. Kametaka, S. Waguri, Author Correction: GGA2 interacts with EGFR cytoplasmic domain to stabilize the receptor expression and promote cell growth, Sci. Rep. 10 (1) (2020) 7675.
[40] T. Uemura, et al., Clathrin adapters AP-1 and GGA2 support expression of epidermal growth factor receptor for cell growth, Oncogenesis 10 (11) (2021) 80.
[41] Y. Contreras-Baeza, et al., Monocarboxylate transporter 4 (MCT4) is a high affinity transporter capable of exporting lactate in high-lactate microenvironments, J. Biol. Chem. 294 (52) (2019) 20135–20147.
[42] H.L. Chen, et al., Aberrant MCT4 and GLUT1 expression is correlated with early recurrence and poor prognosis of hepatocellular carcinoma after hepatectomy, Cancer Med. 7 (11) (2018) 5339–5350.

[43] Y. Zhao, et al., Targeted inhibition of MCT4 disrupts intracellular pH homeostasis and confers self-regulated apoptosis on hepatocellular carcinoma, Exp. Cell Res. 384 (1) (2019), 111591.
[44] S. Li, et al., SUMOylation of PES1 upregulates its stability and function via inhibiting its ubiquitination, Oncotarget 7 (31) (2016) 50522–50534.
[45] W. Xie, et al., Transcriptional regulation of PES1 expression by c-Jun in colon cancer, PLoS One 7 (7) (2012), e42253.
[46] Z. Fu, et al., PES1 in liver cancer: a prognostic biomarker with tumorigenic roles, Cancer Manag. Res. 11 (2019) 9641–9653.
[47] P. Fan, et al., PES1 is transcriptionally regulated by BRD4 and promotes cell proliferation and glycolysis in hepatocellular carcinoma, Int. J. Biochem. Cell Biol. 104 (2018) 1–8.
[48] J.R. Warner, K.B. McIntosh, How common are extraribosomal functions of ribosomal proteins? Mol. Cell 34 (1) (2009) 3–11.
[49] C. Zhou, et al., High RPS11 level in hepatocellular carcinoma associates with poor prognosis after curative resection, Ann. Transl. Med. 8 (7) (2020) 466.
[50] N. Nosengo, Can you teach old drugs new tricks? Nature 534 (7607) (2016) 314–316.
[51] C. Wang, et al., A CRISPR screen identifies CDK7 as a therapeutic target in hepatocellular carcinoma, Cell Res. 28 (6) (2018) 690–692.
[52] M. Zhang, et al., CDK inhibitors in cancer therapy, an overview of recent development, Am. J. Cancer Res. 11 (5) (2021) 1913–1935.
[53] D. Mahadevan, et al., A phase I pharmacokinetic and pharmacodynamic study of AT7519, a cyclin-dependent kinase inhibitor in patients with refractory solid tumors, Ann. Oncol. 22 (9) (2011) 2137–2143.
[54] E.X. Chen, et al., A Phase I study of cyclin-dependent kinase inhibitor, AT7519, in patients with advanced cancer: NCIC Clinical Trials Group IND 177, Br. J. Cancer 111 (12) (2014) 2262–2267.
[55] K.T. Do, et al., Phase 1 study of the HSP90 inhibitor onalespib in combination with AT7519, a pan-CDK inhibitor, in patients with advanced solid tumors, Cancer Chemother. Pharmacol. 86 (6) (2020) 815–827.
[56] K. Karas, et al., Anti-hepatocellular carcinoma activity of the cyclin-dependent kinase inhibitor AT7519, Biomed. Pharmacother. 164 (2023), 115002.
[57] C. Massard, et al., A first in man, phase I dose-escalation study of PHA-793887, an inhibitor of multiple cyclin-dependent kinases (CDK2, 1 and 4) reveals unexpected hepatotoxicity in patients with solid tumors, Cell Cycle 10 (6) (2011) 963–970.
[58] B. Wu, et al., Selected using bioinformatics and molecular docking analyses, PHA-793887 is effective against osteosarcoma, Aging (Albany NY) 13 (12) (2021) 16425–16444.
[59] K. Fan, et al., EZH2 as a prognostic-related biomarker in lung adenocarcinoma correlating with cell cycle and immune infiltrates, BMC Bioinf. 24 (1) (2023) 149.
[60] D. Feng, et al., A gene prognostic index associated with epithelial-mesenchymal transition predicting biochemical recurrence and tumor chemoresistance for prostate cancer, Front. Oncol. 11 (2021), 805571.
[61] J. Zhang, et al., Comprehensive analysis of the glutathione S-transferase Mu (GSTM) gene family in ovarian cancer identifies prognostic and expression significance, Front. Oncol. 12 (2022), 968547.
[62] C. Zheng, Y.D. Tang, The emerging roles of the CDK/cyclin complexes in antiviral innate immunity, J. Med. Virol. 94 (6) (2022) 2384–2387.
[63] S. Goel, et al., CDK4/6 inhibition triggers anti-tumour immunity, Nature 548 (7668) (2017) 471–475.
[64] X. Bai, et al., CDK4/6 inhibition triggers ICAM1-driven immune response and sensitizes LKB1 mutant lung cancer to immunotherapy, Nat. Commun. 14 (1) (2023) 1247.
[65] Y. Chen, Z. Tian, HBV-induced immune imbalance in the development of HCC, Front. Immunol. 10 (2019) 2048.
[66] C.K.Y. Ng, et al., Integrative proteogenomic characterization of hepatocellular carcinoma across etiologies and stages, Nat. Commun. 13 (1) (2022) 2436.
[67] X. Xiao, H. Mo, K. Tu, CTNNB1 mutation suppresses infiltration of immune cells in hepatocellular carcinoma through miRNA-mediated regulation of chemokine expression, Int. Immunopharm. 89 (Pt A) (2020), 107043.
[68] E.J. Lelliott, K.E. Sheppard, G.A. McArthur, Harnessing the immunotherapeutic potential of CDK4/6 inhibitors in melanoma: is timing everything? npj Precis. Oncol. 6 (1) (2022) 26.